Spectral Analysis and Gain Modeling and Numerical Simulation of Bismuth-doped Fiber Amplifier

Kangduo Li [1, *, †], Zihao Wang[2, †], Zhiyu Zhu[3, †]

[1]Department of electronic engineering, North China University of Water Resources and Electric Power, Henan, China

[2] Department of electronic information engineering, Chongqing University of Technology, Chongqing, China

[3] College of optoelectronic engineering, Chengdu University of Information Technology, Chengdu, China

*Corresponding author: 202019319@stu.ncwu.edu.cn

†These authors contributed equally

Abstract: Fiber optic amplifier is an important component of fiber optic communication and the use of the properties of rare earth ions to dope the fiber core is an important way to obtain greater amplification and reduce loss. Because of the unique light-emitting properties of Bismuth ions, the Bismuth doped fiber amplifier (PDFA) has a wide range of applications in the field of fiber amplifier. This paper focuses on the spectral analysis of Bismuth-doped (Bi) fiber amplifiers under different parameters by referring to the absorption spectrum of Bi^{+}. And the energy level structure of Bi^{+} was selected for a wide range of amplification windows $^{3}P_{0}\rightarrow {}^{3}P_{2}$ pumping scheme corresponding to the pumping wavelength of 950 nm, and the rate propagation equation and power transmission equation were established based on the previous work. The numerical simulations were also carried out by MATLAB programming. The effects of doping concentration, fiber length, and pump power on gain, noise index, and output power were analyzed and summarized by MATLAB plotting. In the future, researchers can use neural network algorithms to obtain the combination of Bismuth-doped fiber amplifier parameters that will achieve maximum gain, thus enabling advances in information transmission rates and distances in real-world communications.

Keywords: Fiber Amplifier, Signal Gain, Signal Noise, Bismuth-Doped Fiber.

1. Introduction

Optical fiber is an important communication medium in the current information age. Its principle is to use small and lightweight optical fibers to transmit highly efficient information using light waves as a medium [1]. However, expanding the bandwidth of optical fibers is urgent and demanding. Currently, traditional erbium-doped quartz fiber amplifiers cannot fully utilize the transmission bandwidth of fiber optic communication systems because the effective amplification band is mainly in the C+L band (1530-1610 nm) [2]. Other major fiber laser spectral ranges are also between 1740-2093 and 1160 to 1740nm. Therefore, the spectra in the 1160-1500 nm and 1625-1740 nm ranges are not covered by rare-earth doped fiber lasers, which to some extent affects the development of rare-earth fiber lasers [3].

Bismuth-doped fiber amplifiers have also attracted attention from various countries due to the ultra-broadband amplification properties of Bismuth ions. Since the Bismuth atom has an off-shell electron in a half-full structure, it can form many kinds of ions, such as Bi^{+}, Bi^{4+}, Bi^{5+}, etc.[4], which makes the Bismuth ion can make up for many traditional doped amplifiers such as erbium-doped fiber amplifier (EDFA), Thulium-doped fiber amplifier (TDFA) do not cover the band, and research shows that: the luminescence of Bi ion is affected by many factors, such as covalent bonding, coordination number, lattice symmetry, etc. It has been shown that the luminescence of Bi ions is affected by many factors, such as covalent bonding, coordination number, lattice symmetry, etc. Therefore, Bi ions do not have a distinctive emission spectrum like rare earth ions [5].

Many material workers have worked on developing infrared fiber amplifiers based on Bi ions, using Bismuthate glass as a fiber amplifier matrix material [6] or doping Bi ions into other matrix materials.

In 2001, Fujimoto-to et al. also reported that Bismuth-doped aluminosilicate glass produced ultra-wideband radiation with a peak energy lifetime of 630 ms at 1140 nm and a full half-peak width of 220 nm [7]. Subsequently, they used a $0.8\mu m$ wavelength laser pumping source to achieve light amplification at a wavelength of $1.3\mu m$[8].In 2005, Dianov et al. first fabricated Bismuth-doped optical fibers using a modified chemical vapor deposition technique with a full width at half height of 200 nm and an emission cross-section of up to $6 \times 10^{-21} cm^2$. Subsequently, light amplification and excitation phenomena in the 1300-1500 nm range were observed in Bismuth-doped silicate fibers. Ren et al. studied optical amplification in the continuous wavelength range of 1272-1348 nm in Bismuth-doped germanate glass, so Bismuth-doped fibers are expected to play an important role in future ultra-broadband optical amplifiers [9]. (The bandwidth resources in the ITU standard are largely unexploited and unused, and the development of new broadband optical amplifiers has become a research hotspot in science and industry. Suppose to have independent intellectual property rights in this field and take place. In that case, it is of great significance to improve China's status in the optical communication field [10].

This paper analyzes the Bismuth-doped fiber-optic amplifier and establishes the rate and power transfer equations based on the experimental model. This paper also derive the variation of the amplification gain with fiber length and pump power and the variation of the output power spectrum with pump power and doping concentration through MATLAB programming. The analysis of the effect on the output power was carried out. Starting with the fiber length of 2 m and a doping concentration of $8 \times 10^{-24}$of ASE power versus wavelength and different output power spectra for fiber lengths of 4, 5, 6, and 7 m, as well as the variation of noise index and gain for Bismuth ion doped fibers at different doping concentrations and the variation of gain and noise index with wavelength at different pumping powers. The results show that the parameters such as fiber length and doping concentration can be optimized to achieve better gain and noise index according to this experimental model, which is a guideline in the design and application of Bi-doped fiber amplifiers.

2. Theoretical analysis and modelling

2.1 Theoretical analysis

Before proceeding with the exposition, let me introduce some principles about lasers. When an electron absorbs energy and jumps from a low to a high energy level, the energy is released in the form of a photon, and its optical properties are highly uniform[11]. Due to their monochromatic, directional and high brightness characteristics compared to ordinary light sources. Microscopic particles have a certain energy level structure, and a particle can only be at a certain energy level at any given moment. When a particle interacts with a photon, the particle absorbs or radiates the photon accordingly and jumps to another energy level. When a particle is not excited by an external source, it is in the ground state energy level. When a particle absorbs the energy of a photon, it jumps to a higher energy level and is excited.

Take the two-energy system as an example. The particle receives excitation into the excited state, not the steady state of the particle, such as there can accept the lower energy level of the particle. Even if there is no external excitation, the particle may also spontaneously jump from the high energy level to the lower energy level while radiating a photon of energy $(E_2 - E_1)$, whose frequency is $v = (E_2 - E_1)/h$. This radiation process is called spontaneous radiation. In addition to spontaneous radiation, particles at the higher energy level E2 can also leap to lower energy levels in another way. When the frequency is $v = (E_2 - E_1)/h$, it is also possible for a particle to leap from energy level E_2 to energy level E_1 and simultaneously radiate two photons with the same frequency, phase, polarisation state and direction of propagation as the foreign photon, a process known as stimulated radiation.

The concept of excited radiation is based on a new theory proposed by Albert Einstein in 1916. It states that due to the excitation of some photons, particles will jump from higher energy levels to lower energy levels and excite or radiate light, which has the same nature as the light that started the leap is stimulated or emitted during the leapfrogging process. Under special conditions, there is also the phenomenon of weak light exciting strong light, a process that reflects the concept of light amplification by stimulated radiation, which can be abbreviated to laser [12]. In the case of matter in general, the three processes of spontaneous radiation, stimulated absorption and stimulated radiation are always taking place simultaneously. Under normal circumstances, the number of atoms in the lower energy levels is always greater than in the higher energy levels. As a rule, the probability of spontaneous radiation is significantly greater than that of excited radiation, since spontaneous radiation can take place under any conditions [13]. A fiber laser consists mainly of a pump source, a resonant cavity and a gain fiber. The pump source is the excitation source that enables the laser working medium to reach particle number reversal. The jump of the particles from the ground state to the higher energy levels is called the pumping process. The resonant cavity is an important component of a fiber laser, providing positive feedback, limiting the direction and frequency of the beam, and controlling the output power and energy. Resonant cavities are divided into Fabry Perot, ring, and “8” shaped cavities. Gain fibers are doped with rare-earth elements, such as Nd^{3+}, Yb^{3+}, $Er^{3+}$and Tm^{3+} [14].

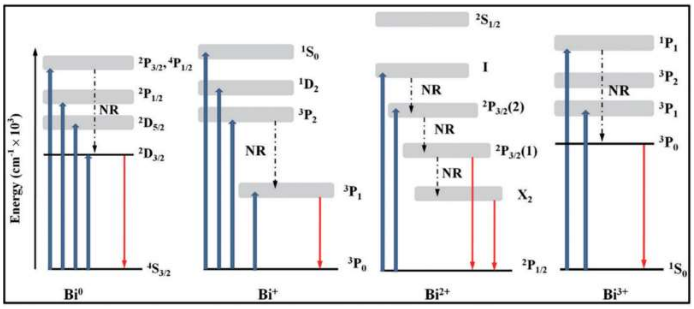

Figure 1. Energy level diagram of Bismuth ions (Bi^0, Bi^+, $Bi^{2+}$and Bi^{3+}) [15]

The excitation spectra of the electron transitions from $^3P_0\rightarrow {}^1S_0$, $^3P_0\rightarrow {}^1D_2$, $^3P_0\rightarrow {}^3P_2$ and $^3P_0\rightarrow {}^3P_1$ of $Bi^+$are located at 320 nm (31250 cm^{-1}), 500 nm (20000 cm^{-1}), 700 nm (14000 cm^{-1}), and 1000 nm (10000 cm^{-1}), respectively, and their NIR emission spectra are derived from the $^3P_1\rightarrow {}^3P_0$ electron transitions of Bi^+ [15].

Bi has a variety of ionic forms. This paper mainly focuses on the analysis of +1 valence Bismuth ion, according to the truncation method measured by Ming-Sheng Cheng et al. [9] to obtain the absorption spectrum of their homemade Bismuth-doped fiber.1 Bi^+ has a variety of excitation schemes such as Figure 2 shows the energy level structure of Bi^+ and the corresponding pumping wavelength, the excitation scheme can be selected according to the wavelength band to be analyzed. This paper mainly focuses on the analysis of the 1200-1600 nm band spectrum. This paper focuses on the spectral analysis in the 1200-1600 nm band, so this paper choose the three-level scheme of $^3P_0\rightarrow {}^3P_2$ excited state $^3P_2$ to the sub-stable state $^3P_1$ and $^3P_1$ energy level particles finally leap back to $^3P_0$ energy level.

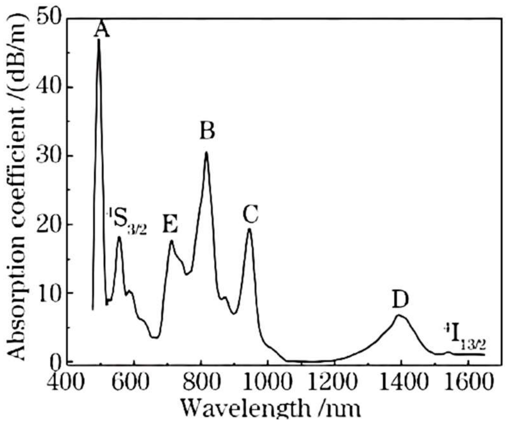

Figure 2. The absorption spectrum of Bismuth-doped fiber measured by Cheng Mingsheng et al [9]

The A, B, C, and D bands in Figure 2 correspond to the excited states ${}^1S_0$, ${}^1D_2$, ${}^3P_2$, ${}^3P_1$, which correspond to wavelengths of 500 nm, 820 nm, 950 nm and 1400 nm, respectively. In addition, the E band at a central wavelength of around 700 nm is produced by a Bismuth particle, and the absorption bands at 550 nm and 1540 nm corresponding to the atomic states of erbium particles ${}^4S_{3/2}$ and ${}^4I_{3/2}$, respectively.

2.2 Modeling

In the steady-state case, the excited absorption rate R_{12} is equal to the excited radiation rate R_{21}. The equation for the excitation absorption rate and the equation for the excitation radiation rate can be written as:

$$R_{12} = B_{12}N_1\rho(hv) \tag{1}$$

$$R_{21} = A_{21}N_2 + B_{21}N_2\rho(hv) \tag{2}$$

where B_{12} is the Einstein absorption coefficient, N_1 is the number density of particles at the lower energy level. A_{21} is the probability of spontaneous radiation jumping, B_{21} is the Einstein emission coefficient, and N_2 is the number density of particles at the upper energy level. $\rho(hv)$ is the number of photons per unit time per unit area, A_{21} is the probability that an atom in energy state 2 will spontaneously fall to a lower energy state 1 and emit a photon of energy $h\omega$ per unit time. B_{21} denotes the rate of a leap to a higher energy level by absorbing a photon $h\omega$ when energy-dense W radiation is present, proportional to $W(\omega)$ with a scale factor B_{12}, i.e. leap rate $\psi = B_{12}W(\omega)$. B_{21} is in contrast to B_{12}, the rate of the leap from state 2 to state 1 is also proportional to $W(\omega)$ with a scale factor B_{21}, i.e., leap rate $\psi = B_{21}W(\omega)$, called induced or excited emission. Explicitly the three Einstein coefficients A_{21}, B_{12} and B_{21}, only need to consider the nature of the two atomic states, independent of $W(\omega)$ [16].

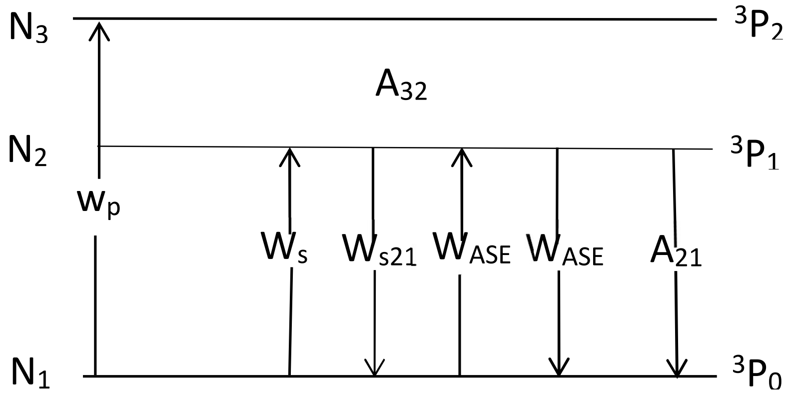

Figure 3. Schematic diagram of the three-energy level structure

According to the selected pumping scheme, the energy level jumping process can be simplified to a three-energy level structure, as shown in Figure 2. The rate equation in the computational model for the output power of the spontaneous emission spectrum of the Bismuth-doped fiber amplifier studied in this paper can be written as

$$\frac{\partial N_1(z)}{\partial t} = -[W_P(z) + W_{12}(z)]N_1(z) + A_{21}N_2(z) + W_{21}(z)N_2(z) \quad (3)$$

$$\frac{\partial N_2(z)}{\partial t} = W_{12}(z)N_1(z) - A_{21}N_2(z) - W_{21}(z)N_2(z) + A_{32}N_3(z) \quad (4)$$

$$\frac{\partial N_3(z)}{\partial t} = W_P(z)N_1(z) - A_{32}N_3(z) \quad (5)$$

$$N = N_1(\mathrm{z}) + N_2(\mathrm{z}) + N_3(\mathrm{z}) \quad (6)$$

$$W_P(z) = \frac{\sigma_{13}P_p(z)}{hv_{13}A_{eff}} \quad (7)$$

$$W_{12}(z) = \frac{\sigma_{12}(v_{12})P_s(z)}{hv_{12}A_{eff}} \quad (8)$$

$$W_{21}(z) = \frac{\sigma_{21}(v_{21})P_s(z)}{hv_{21}A_{eff}} \quad (9)$$

$$A_{eff} = \pi r^2 \quad (10)$$

In Eq. (3), the partial derivative of N_1 with respect to time is proportional to the product of the pump light and the spontaneously emitted light added to N_1, $A_{21}N_2(z)$ represents spontaneous radiation, electrons from the second energy level to the first energy level, electron radiation causing an increase in electrons on N_1, $W_{21}(z)N_2(z)$ represents the excited radiation of the signal light. In Eq. (4), the simultaneous decrease in N_1 and increase in N_2 with time, the electron leaps to N_2, A_{32} represents the electron moving from the third energy level to the second energy level, and the product of A_{32} and N_2 represents the number of times per second the electron moves from the three energy levels to the second energy level. Also in Eq. (5), the simultaneous increase in N_3 and decrease in N_2 with time. In Eq. (7) W_P represents the number of times per second that the pump light excites an electron from the ground state to the third energy level, proportional to the pump power P_P, the rest of the physical quantities are constants. In Eqs. (8) and (9), the absorption of spontaneous emission light excites the electrons from the ground state to the second energy level. During the absorption of spontaneous emission light, when the spontaneous emission light is transmitted forward, it has the potential to stimulate the electrons in the second energy level to produce excited emission and amplification. Equation (10) is the formula for the area of an optical fiber.

Its power propagation equation can be written as

$$\frac{dP_P(z)}{dz} = \left(-\sigma_p N_1(\mathrm{z}) - \alpha_p\right)P_P(z) \quad (11)$$

$$\frac{dP_s(z)}{dz} = [\sigma_{21}N_2(\mathrm{z}) - \sigma_{12}N_1(\mathrm{z}) - \alpha_s]P_s(z) \quad (12)$$

$$\frac{dP_{ase}(z)}{dz} = [\sigma_{21}N_2(\mathrm{z}) - \sigma_{12}N_1(\mathrm{z}) - \alpha_s]P_{ase}(z) + 2\sigma_{21}N_2(\mathrm{z})hv\Delta v \quad (13)$$

The variation of pump power, signal power, and ASE power with propagation length is called the power propagation equation, and equation (11) is negative due to the absorption of pump light from the ground state to the excited state and $\frac{dP_P(z)}{dz}$ is proportional to $\sigma_p N_1(\mathrm{z})$ is proportional to. The signal light in equation (12) is amplified by the excited radiation corresponding to $\sigma_{21}N_2(\mathrm{z})$ is positive and the negative absorption corresponds to $\sigma_{12}N_1(\mathrm{z})$ The amplification depends on whether the former value is greater than the latter value. In equation (13) $2\sigma_{21}N_2(\mathrm{z})hv\Delta v$ represents the forward and backward propagation of light from the newly generated spontaneous radiation. The meanings and units of the parameters of the propagation equation are given in Table 3

Table.1. Parameters of the power propagation equation

Parameter name	Meaning	Unit
$P_P(z)$	Pumping power	W
$P_s(z)$	Signal power	W
$P_{ase}(z)$	ASE power	W
α	Loss factor of fiber optic materials	$/m$
Δv	Frequency half-height full width	Hz

The following is the second and third part of the simulation analysis of the equations relating to the counting amplification and gain, in addition to the introduction of a noise index to analyze the variation of the signal-to-noise ratio of the fiber amplifier at different bands

$$A(P_P(z), P_s(z), N_2, N_1, z) = \frac{P_s(z)}{P_s(0)} \tag{14}$$

$$G(P_P(z), P_s(z), N_2, N_1, z) = 10log10\left(\frac{P_s(z)}{P_s(0)}\right) \tag{15}$$

$$\text{Fs} = 10\text{lg}\left(\frac{\text{Pase(z)}}{\text{h}vG\Delta v} + \frac{1}{\text{G}}\right) \tag{16}$$

Table.2. Parameters of the gain equation

Parameter name	Meaning	Unit
A	Magnification	%
G	Gain	dB
Fs	Noise index	dB
h	Planck's constant	$J \cdot s$

The pump light absorption rate, the spontaneous emission light absorption rate, and the spontaneous emission light excited radiation rate are all affected by the propagation length z. From the equation, it can obtain the pump light absorption rate, the spontaneous emission light absorption rate, and the spontaneous emission light excited radiation rate. Therefore, it is the ode45 function and the function in Matlab to calculate the above equations.

3. Experimental procedure

By programming the model with MATLAB software, the first part analyzes the effect on the output power from a total of three parameters of the optical fiber transmission, assuming that at A_{eff} is $10\mu m^2$, A_{21} is 1000 times/s, A_{12} is 10^6 times/s, the background loss of the pump light (α_p) and the background loss of the signal light (α_s) were both $0.1m^{-1}$ In this step, Newton's iteration can be used to increase the speed of operation. Still, since each step requires the inverse of the Hessian matrix of the objective function, it increases the amount of operation. Since the left end of equations (3-5) is zero in the steady state case, it is convenient to use the symbolic solution for substitution. Therefore, the symbolic solution method is preferred for the solution.

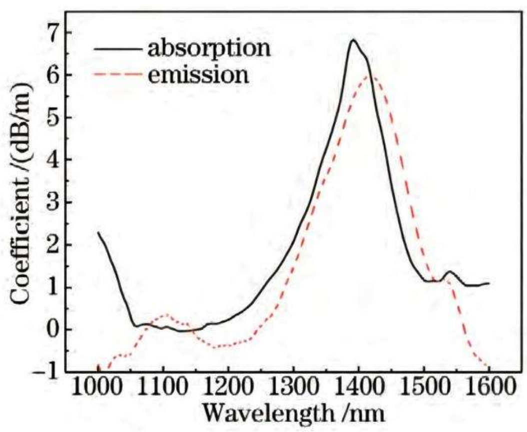

Figure 4. shows the absorption and emission spectra measured by Cheng Mingsheng et al. [9]

Figure 4 shows the absorption and emission spectra measured by Cheng Mingsheng [9]. The solid black line is their experimentally measured absorption spectrum with a peak absorption wavelength at 1375 nm, the absorption peak at 1375 nm is due to the combined effect of the hydroxide ion vibration and the active Bismuth center. The red dashed line is the radiation spectrum of the doped fiber under 830 nm pumping with a central wavelength at 1420 nm. a radiation peak at 1540 nm occurs due to the action of the erbium ion. In order to simulate the emission and absorption spectra of the Bismuth ions in the main program, this paper invoked the creation of two normal distribution functions with intermediate values of 1375 and 1420, respectively, it could combine the unknown σ_{12} and σ_{21} defined as the normalization of the dependent variable y of the probability density function i.e.

$$\sigma = \left[\frac{y}{\max(y)}\right] \times 10^{-24} \tag{17}$$

In literatures, the normalizing property of the integration of the probability density function over the space of random variable values to 1 has not been independently proposed. Still, it has been used in much of the literature to calculate integrals. The normalization condition of the Gamma distribution was used by Han Ming [17] to calculate the posterior density of the failure rate of failure-free data. And the normalization condition of the Beta distribution was used to calculate the Bayes estimate of the reliability of failure-free data. In particular, the concept of a kernel defining the probability density of a random variable is based on the normalization condition of the probability density.

In addition, in order to study the changing wavelength λ and the changing σ_{12} and σ_{21} need to use the for loop multiple times with ode45, this paper added multiple for loops to compare the variation in output power at different doping concentrations, fiber lengths, and pump powers.

The second part analysis the correlation law based on the first part using the ODE45 function [18] by programming the equations of the fiber length z versus gain G, signal power P_s, pump power P_p, and ASE power.

In the third part, based on the first two parts, the two parts are fused to obtain the variation of amplification and noise index with signal wavelength for different pumping powers, different fiber lengths, and different doping concentrations so as to analyze the amplification effect of the fiber amplifier on the signal and its loss.

4. Results and Discussion

4.1 Output power spectral analysis

Table.3. Parameters used for simulation

Parameter name	Value	Unit
Speed of light (c)	3×10^8	m/s
Planck constant (h)	6.626×10^{-34}	$J \cdot s$
Pump light background loss α_p	0.1	m^{-1}
Signal light background loss α_s	0.1	m^{-1}
Pump light overlap factor Γ_p	0.856	
Signal light overlap factor Γ_s	0.514	
Fiber radius r	1.5×10^{-6}	m
Chance of radiation leap A_{21}	1000	$/s$
Radiation-free jump rate A_{32}	1×10^6	$/s$

The parameters used in the simulations are simplified here. Γ_s and Γ_p are the overlap factors of the signal light and pumping light mode fields and the doped ions in the core, respectively [10]. According to the physical properties of the energy level leap, particles tend to leap from higher to lower energy levels. The chance of a radiation leap is generally much smaller than that of a no radiation leap. So the no radiation leap is set to 1000 times the radiation leap in the simulation. Since this is an idealized model, the background loss depends mainly on the cladding and other components of the fiber, and here the simulations are set to $0.1m^{-1}$.

A total of four images were obtained through MATLAB programming, firstly Figure 5 shows the most basic initial ASE power of 0, fiber length of 2m, doping concentration of 8×10^{24} The ASE power versus wavelength for an initial pumping power of 200 mW

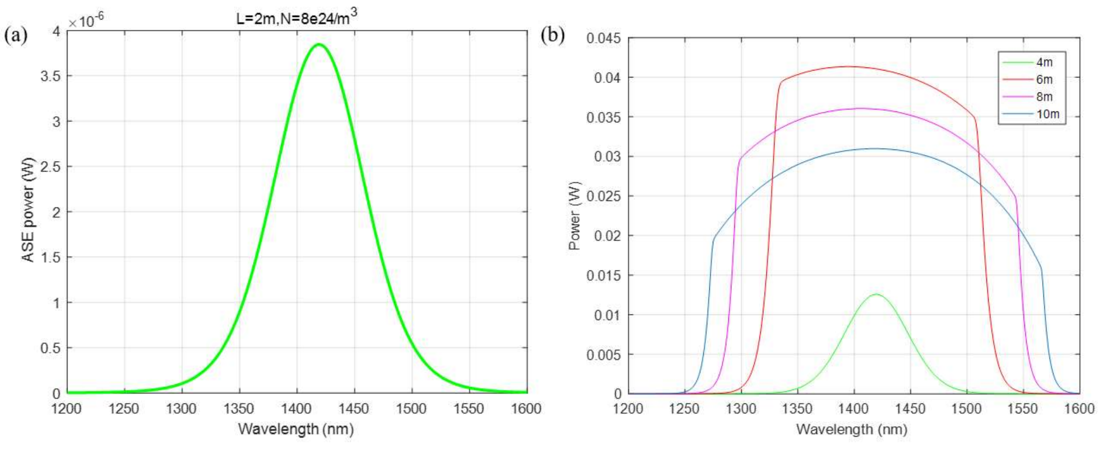

Figure 5. ASE power and Output power versus wavelength

Based on the images it can be seen that the ASE power trends as a Dirac (δ) function between 1200 and 1420, which basically converges to the simulated Bismuth ion absorption spectrum of the setup, and peaks at 1420 nm with the ASE power close to 4×10^{-6}. The ASE power is close to 1420 nm and decreases rapidly afterward, depending on the energy leap scheme this paper have chosen $^3P_0 \rightarrow {}^3P_2$ excited state with a central wavelength of 1420 nm.

In Figure 5(B), the prerequisite conditions are a doping concentration of 8×10^{24}. The peak output power increases significantly with increasing fiber length in the 4-6m fiber length range, with 6m being the most suitable but decreasing significantly in the 6-10m range. Still, the amplification bandwidth at 6m is narrower than larger fiber lengths, and the range of application is reduced. The range of applications is also reduced. As the wavelength grows to a certain point, it reaches a rising turning point. Then as the wavelength grows the output power grows slowly to a peak and then decreases gradually, before reaching a falling turning point, a characteristic that reflects the windowing nature of amplification within a certain wavelength range.

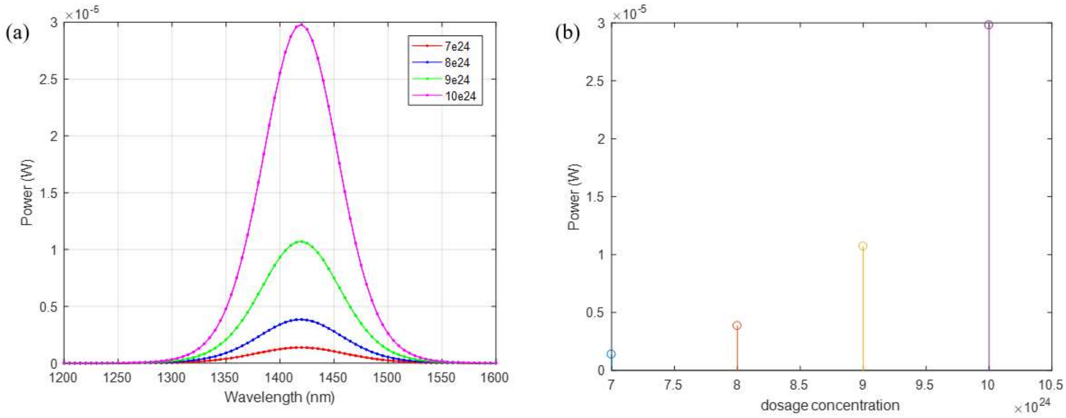

Figure 6. Output power spectrum and trend of output power maximum with doping concentration for different doping concentrations

Figure 6 shows the output power spectrum of a fiber with a fiber length of 2m and an initial pump power of 200mW Bismuth ion-doped fiber at different doping concentrations. Four doping concentrations were selected in the experiment as 7×10^{24}, 8×10^{24}, 9×10^{24} and10×10^{24}. The output power maximum with doping concentration can be seen in the image of the trend of the doping concentration of 10×10^{24} The maximum growth rate of the output power peak at the doping concentration is 3×10^{-5}. According to the peak stick figure, the peak output power increases by 217% as the doping concentration increases from 7×10^{24} to 10×10^{24}.

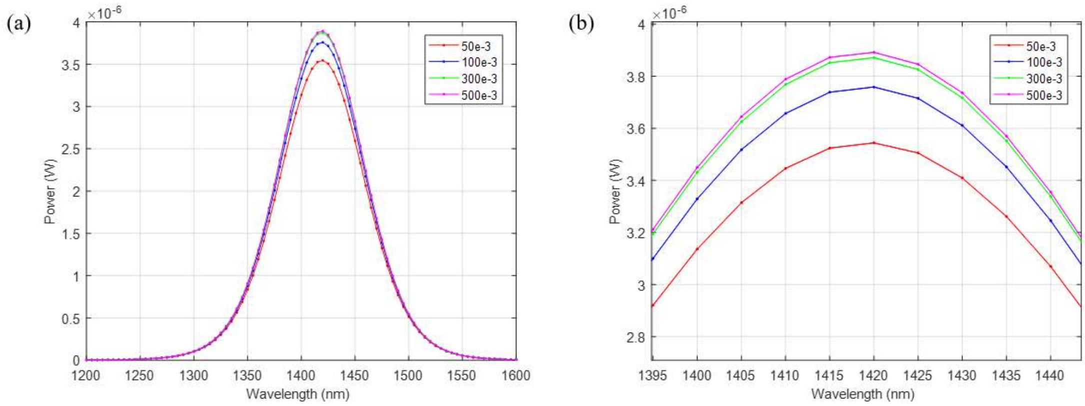

Figure 7. Output power spectrum for different pump powers and top amplification

Figure 7 shows the output power spectrum for a fiber length of 2m with a doping concentration of 8×10^{-24}. From the figure 7, as the pump power increases the output power increases, verifying that the pump power determines the degree of particle number inversion and hence the gain. However, increasing the pump power is not an effective way to increase the output power, as the image shows that the output power stops rising when the pump power reaches 300mW.

4.2 Gain and associated power analysis of with fiber length

On the basis of the previous section, other parameters were fixed for the analysis of the fiber length, and the other parameters were doping concentration of 2×10^{24}. The initial pumping power is 200mW signal power at the input of the fiber 1×10^{-6}W.

Other conditions:

Table.4. Parameters used for calculations

Parameter name	Value	Unit
Speed of light c	3×10^8	m/s
Planck constant h	6.626×10^{-34}	$J \cdot s$
Pump light background loss α_p	0.1	m^{-1}
Signal light background loss α_s	0.1	m^{-1}
Pump light overlap factor Γ_p	0.856	
Pump light overlap factor Γ_s	0.514	
Fiber radius r	1.5×10^{-6}	m
Radiation leap rate A_{21}	1000	$/s$
Radiation leap rate A_{32}	1×10^6	$/s$
ASE spectral width	2×10^9	Hz

The following diagram was obtained by simulation.

The relationship between fiber length and gain can be analyzed in Figure 8(a). Firstly, it is obvious that when the fiber length rises sharply in the range of A- to B-point, it peaks at around 1.2 m. Beyond 1.2 m, the gain slowly decreases, and in the 1.2-8.5 is the slow decline zone at 7.339 m. It decreases by 29.4% at this stage. After that, it decreases by 70.6% at 1.17 m. The gain is only positive at 0-9.8 m. This means this fiber amplifies significantly at 0-9.8 m. The gain is only positive at 0-9.8m, which means that this fiber has a significant amplification effect at 0-9.8m.

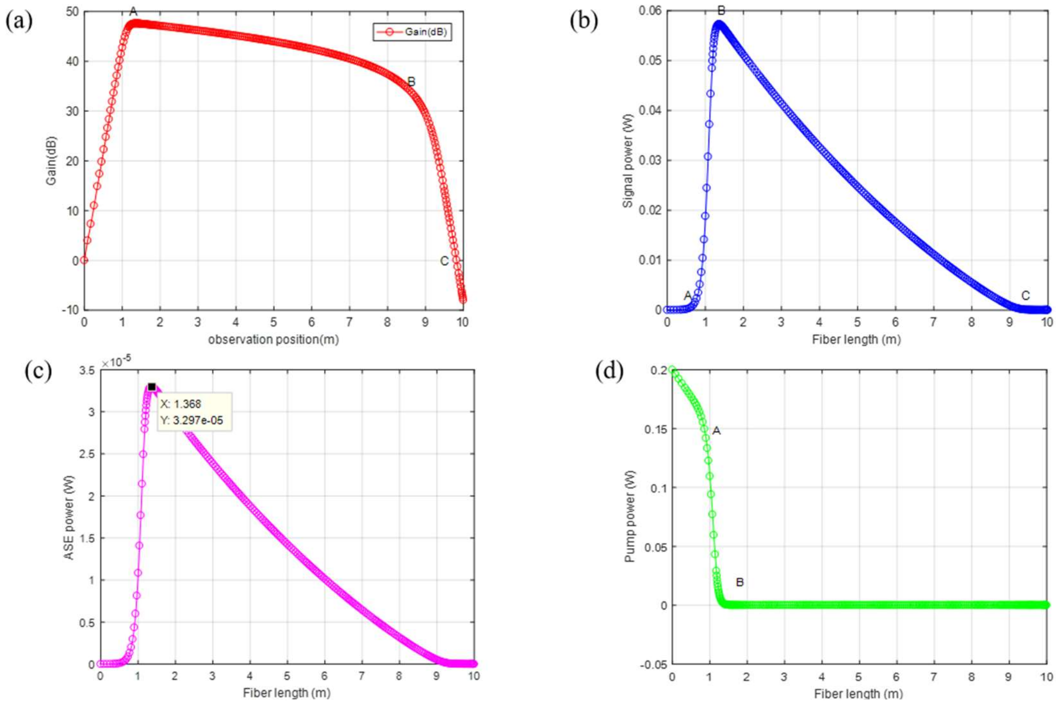

Figure 8. Effect of fibre length on fibre parametres

(a) Fiber length versus gain (b) Fiber length versus signal power

(c) Fiber length versus ASE power (d) Fiber length versus pumping power

The above three graphs show the relationship between fiber length and signal, ASE and pump power. The ASE power and b-signal power have similar trends, both rising rapidly in the early stages to reach a peak at around 1.35 and then slowly decreasing to 0 at around 9.2 m, while 9.2 m is also the position where the gain drops sharply. The fiber length and pump power have a decreasing relationship, starting to accelerate at around one metre with a slope of -0.27, dropping to 1.5 W at 1.37 m before converging to 0.

4.3 Gain and S/N ratio analysis with two other parameters

The third part analyses the pump power, doping concentration for gain G and noise index Fs. In this part the independent variables are replaced by wavelengths to show the correlation more intuitively. Firstly, this paper compare the effect of different pumping power on gain and noise at different wavelengths, and in this section, set the input signal power to 1×10^{-4}W At a fiber length of 2 m and a doping concentration of 6×10^{24}, the discussion is carried out.

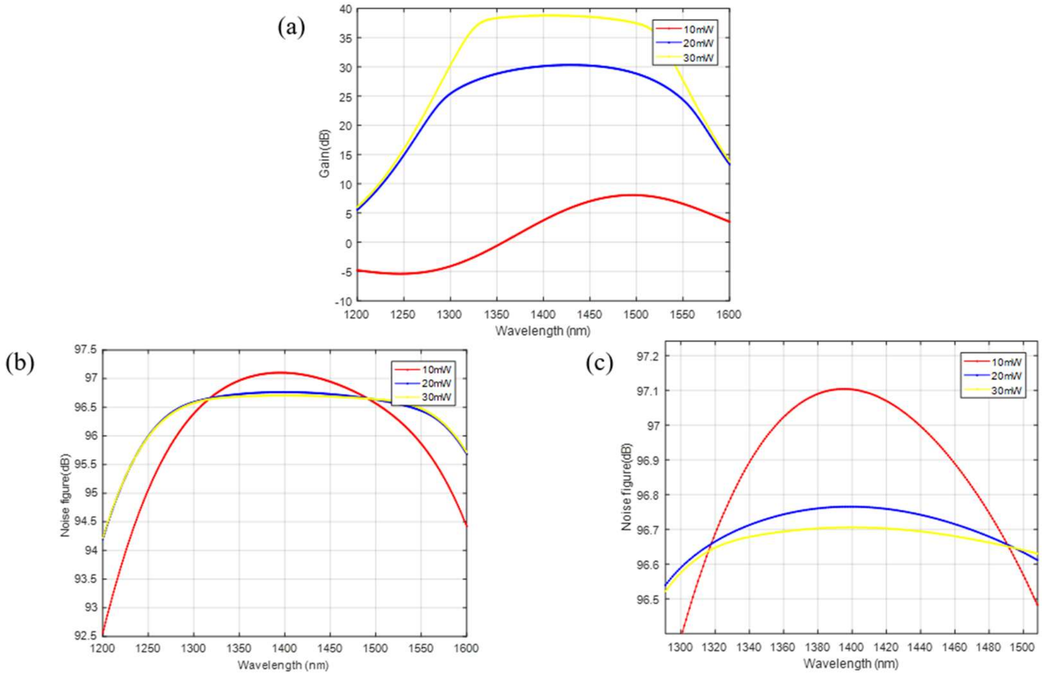

Figure 9 Effect of pump power on gain and noise index at different wavelengths

(a) Variation of gain with wavelength at different pump powers

(b) Variation of noise index with wavelength at different pump powers

(c) Variation of noise index local magnification

Figure 9 (a) shows that lower pump power requires amplifying wavelengths in a certain range at higher doping concentrations. The amplification is very low, and the maximum gain is also around 10. In contrast, higher amplification can achieve full-band amplification of 1200-1600 nm. The highest amplification is reached at the absorption peak around 1400 nm, while each pump power case in Figure 9 (b) shows the variation of the noise index. The noise index is opposite to the gain. The higher the pump power, the lower the peak noise index, which is a feasible solution to improve the signal to noise ratio.

Next, the variation of gain and noise index for different doping concentrations, under the condition of 930 nm pumped optical power 0.1W and the fiber length remains 2 m.

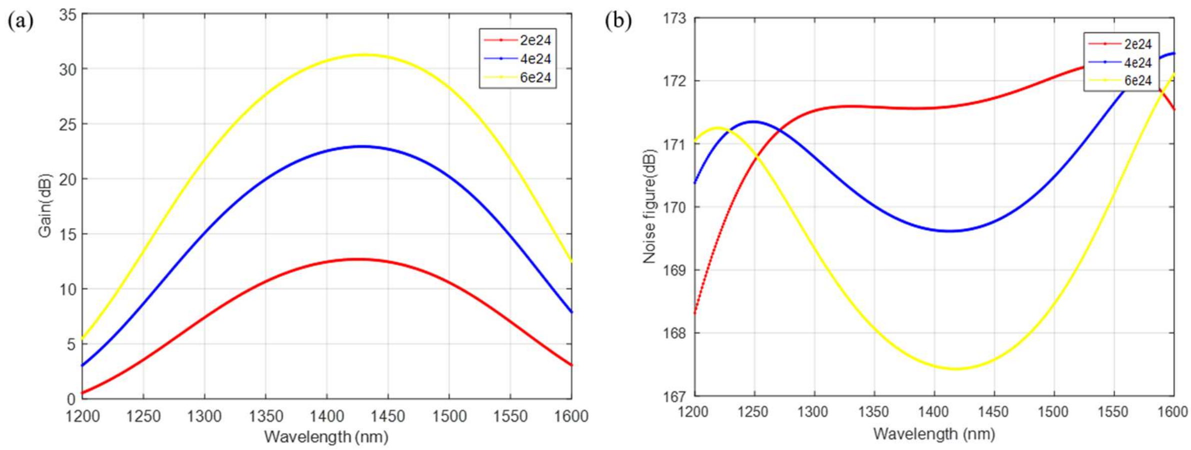

Figure 10. Effect of doping concentration on gain and noise index at different wavelengths

From the images, the doping concentration has similar properties to the pump light. Again the gain increases with increasing doping concentration, and the noise index decreases with increasing doping concentration. Generally, the higher the gain, the lower the noise index. A higher gain means that the signal light consumes a higher number of excited state particles, so ASEs competing with the signal light for gain are therefore suppressed.

5. Conclusion

In this paper, Bismuth-doped optical fibers amplify at higher amplification levels in the full band of 1200-1600 nm, and the highest amplification is achieved at the absorption peak around 1400 nm. The emission and absorption spectra of Bismuth-doped fibers are simulated to study the output power variation at different doping concentrations, fiber lengths, and pump powers. The relationship equations between fiber length z and gain G, signal power P_S, pump power P_P and ASE power were established and the correlation laws were analyzed. The variation of amplification and noise index with signal wavelength for different pump powers, different fiber lengths and different doping concentrations were obtained to analyze the amplification effect of the fiber amplifier on the signal and its loss.

In recent years, the simulated annealing algorithm has been widely used as a general-purpose stochastic search algorithm for nonlinear solution problems in various fields. In the next step, numerical optimization of fiber pumping power, output power, doping concentration, fiber length, relaxation coefficient, and core cross-sectional area can be performed by a simulated annealing algorithm or genetic algorithm based on this paper [19].

References

[1] Wang F. Development of doped fiber amplifiers and their applications [J]. China New Communication,2018,20(06):80.

[2] Wang Fugang. “Research on Optical Properties of Bismuth-Erbium Co-Doped Silica Fiber: Beijing University of Posts and Telecommunications”cnki, January 9, 2015.

[3] Yevgeny Dyalov. “History development and prospects of Bismuth-doped optical fibers”cnki, February10, 2020.

[4] Jia Baonan, Wang Fu Gang, Sun Shihao, Liu Gang, Lu Pengfei. “Research progress on the luminescence mechanism of Bismuth-doped optical fibers with Bismuth active centres”.cnki November 11, 2020.

[5] ZHAO Yanzhao, GAO Lewen, GU Xianwen, GUO Wenji “Progress in the study of near-infrared fluorescence properties of Bismuth-doped glass materials” cnki, May 15,2013.

[6] S.H. Jin, Y.F. Qin, X.J. Wang, H.P. Xia, “Study of novel Bismuth-doped substrate materials for broadband amplifiers”Natural Science, 2008.

[7] Fujimoto, M Nakatsuka. Infrared luminescence from Bismuth-doped silica glass[J]. Jpn J Appl Phys, 2001, 40: L279-L281.

[8] Peng Mingying, Wang Chen, Qiu Jianrong, Meng Xiankang, Chen Danping,Jiang Xiongwei, Zhu Congshan. "New Bismuth-doped light-emitting materials for ultra-wideband fiber amplifiers"cnki, Decmeber 20, 2005.

[9] Cheng Mingsheng, Yan Cellophane, Sang Xinzhu, Wang Kwairu, Yuan Jinhui, Yu Chongxiu, Luo Yanhua, Peng Gangding, Jia Changxin. "Study on broadband optical amplification characteristics of Bismuth-doped optical fiber"

[10] Zhou Shi-Feng, Qiu Jian-Rong. Ultra-broadband optical amplification of novel Bismuth-doped glasses[J]. Chinese optics 2007: 29.

[11] Gu Bo. "Current status and application development trend of laser processing technology and industry".cnki, October 01, 2020.

[12] Yang Zhou. "Research on the principle and application of laser technology[J]. Information Communication" cnki, March 15, 2014.

[13] Zhang Weijian. "Basic principles of laser and medical applications[J]. Scientific Advisory (Science and Technology - Management)" cnki , August 05, 2011.

[14] Zhang Zuxing, Zhou Xia Bing. "Practical exploration of "laser principle" research study Educational Teaching Forum" cnki, March 24, 2021.

[15] Chen ting, Cao renping "Advances in Bismuth ion luminescence research" cnki, August 10, 2021.

[16] Lu Jinan "The classical description of Einstein coefficients in quantum optics" cnki, June 10, 2003.

[17] Tan Luyun,Cheng Weimin "The application of probability density function of random variables in integral science" cnki, June 15, 2007.

[18] Liu Shihong "Gain and noise index calculation and procedure for praseodymium-doped fiber amplifier" China Broadband,2022,18(5):104-106

[19] Zhang Bo. "Optimization of Thulium-doped fiber laser characteristics basedon genetic algorithm"cnki, March 21, 2018.